Melanoma differentiation associated gene-7/interleukin-24 reverses multidrug resistance in human colorectal cancer cells

Luni Emdad,[1,2] Irina V. Lebedeva,[1] Zao-Zhong Su,[1] Devanand Sarkar,[1,3] Paul Dent,[4] David T. Curiel,[5] and Paul B. Fisher[1,2,3]

Departments of [1]Urology, [2]Neurosurgery, and [3]Pathology, Herbert Irving Comprehensive Cancer Center, Columbia University Medical Center, College of Physicians and Surgeons, New York, New York; [4]Departments of Biochemistry and Radiation Oncology, Virginia Commonwealth University, Richmond, Virginia; and [5]Division of Gene Therapy, Departments of Medicine, Pathology and Surgery, and the Gene Therapy Center, University of Alabama, Birmingham, Alabama

Abstract

Overexpression of the *multidrug resistance 1* (*MDR1*) gene, encoding P-glycoprotein (P-gp), facilitates resistance to diverse chemotherapeutic drugs and current P-gp inhibitors display high toxicity. We studied the effects of melanoma differentiation associated gene-7/interleukin-24 (*mda*-7/IL-24), which exhibits cancer-specific apoptosis-inducing properties, in drug-sensitive (SW620) and drug-resistant (SW620/Dox) colorectal carcinoma cells. Adenovirus administered *mda*-7/IL-24, Ad.*mda*-7, effectively reversed resistance to doxorubicin-induced apoptosis in SW620/Dox cells by increased intracellular accumulation and decreased efflux of doxorubicin. Unexpectedly, P-gp–overexpressing cells (SW620/Dox) displayed increased apoptosis following Ad.*mda*-7 infection compared with parental SW620 cells, which correlated with more MDA-7/IL-24 protein in SW620/Dox than SW620 cell and potentially explains the increased sensitivity of P-gp–overexpressing cells to *mda*-7/IL-24. Transient overexpression of *MDR1* in SW620 cells significantly increased apoptosis, decreased anchorage-independent growth, and increased MDA-7/IL-24 protein following Ad.*mda*-7 infection, whereas down-modulation of *MDR1* in SW620/Dox cells by small interfering RNA decreased apoptosis following Ad.*mda*-7 infection. The increased *mda*-7/IL-24 sensitivity observed in SW620/Dox cells was partly due to increased reactive oxygen species generation and lower mitochondrial membrane potential. These findings confirm that *mda*-7/IL-24 is a potent MDR reversal agent, preferentially causing apoptosis in P-gp–overexpressing MDR cells, suggesting significant expanded clinical implications for the use of *mda*-7/IL-24 in treating neoplasms that have failed chemotherapy mediated by the P-gp MDR mechanism. [Mol Cancer Ther 2007;6(11):2985–94]

Introduction

Resistance to cytotoxic agents in tumor cells is one of the most serious obstacles to successful anticancer chemotherapy (1). Cancer cells can become resistant to a single drug or to a family of drugs with identical mechanisms of action. Alternatively, they may also acquire broad cross-resistance to mechanistically and structurally unrelated drugs, a phenomenon known as ''classic'' multidrug resistance (MDR). MDR is a significant impediment to effective cancer chemotherapy in many patients and a major mechanism underlying resistance of cancer cells to diverse chemotherapeutic agents (2). An accepted mechanism of MDR is a reduced cellular accumulation and an altered subcellular distribution of cytotoxic drugs. Of the 48 human ATP-binding cassette transport proteins (3), P-glycoprotein (P-gp; a product of the *MDR1/ABCB1* gene) is the best-known and principal mediator of MDR (4, 5). The first mechanistic insights into P-gp–induced resistance came from the cloning of *MDR1* and from confirmation of sequence homology between P-gp and bacterial ATP-binding cassette transport proteins (5, 6). Introducing the *MDR1* gene exogenously through a gene transfer approach has also established a direct functional association between P-gp overexpression and the MDR phenotype (7). P-gp is capable of pumping several structurally unrelated chemotherapy drugs and other compounds out of the cell by using the energy of ATP hydrolysis (8–10), which results in decreased intracellular accumulation of compounds and hence resistance to drug cytotoxicity. Innate or acquired expression of P-gp, therefore, is a significant problem in cancer chemotherapy and successful inhibition of P-gp transporter function or its expression may overcome the MDR phenotype by increasing intracellular accumulation of anticancer drugs.

Several *in vitro* and *in vivo* studies have been done to reverse the drug resistance phenotype and to develop innovative chemotherapeutic strategies effective against MDR tumors. Among the P-gp inhibitors, calcium channel

Received 6/13/07; revised 8/31/07; accepted 9/27/07.

Grant support: NIH grants R01 CA097318, R01 CA098712, and P01 CA104177; Samuel Waxman Cancer Research Foundation; and Chernow Endowment. P.B. Fisher is the Michael and Stella Chernow Urological Cancer Research Scientist and a Samuel Waxman Cancer Research Foundation Investigator.

The costs of publication of this article were defrayed in part by the payment of page charges. This article must therefore be hereby marked *advertisement* in accordance with 18 U.S.C. Section 1734 solely to indicate this fact.

Requests for reprints: Paul B. Fisher, Departments of Pathology and Urology, Columbia University, College of Physicians and Surgeons, 630 West 168th Street, New York, NY 10032. Phone: 212-305-3642; Fax: 212-305-8177. E-mail: pbf1@columbia.edu

doi:10.1158/1535-7163.MCT-07-0399

blocker (verapamil), which has a potent effect on reversal of MDR through inhibition of P-gp, was the first (11). Subsequently, several other structurally unrelated compounds, such as calmodulin inhibitors (e.g., trifluoperazine) and immunosuppressive agents (e.g., cyclosporine A), have also been shown to be effective inhibitors of P-gp (12, 13). However, Phase III clinical trials have been disappointing, and no survival benefit of P-gp inhibition has yet been achieved (14, 15). In fact, there are currently no reversal agents clinically available.

A major reason for this lack of clinical success arises from the deleterious effects of the reversal agents on normal tissues expressing P-gp and their intrinsic toxicities *in vivo*. Consequently, development of potent yet selective P-gp inhibitors with a low degree of undesirable side effects is gaining interest in clinical oncology. In this context and based on the current studies, melanoma differentiation-associated gene-7/interleukin-24 (*mda*-7/IL-24) might be a preferable candidate to achieve this end point. Initial studies focused on the growth-inhibitory properties of this molecule, resulting in the provocative observation that *mda*-7/IL-24 selectively suppresses the growth of a broad spectrum of tumor cells without affecting growth of normal cells (16, 17). When administered by a replication-incompetent adenovirus (Ad.*mda*-7), *mda*-7/IL-24 exhibited nearly ubiquitous antitumor properties *in vitro* and *in vivo*, leading to its rapid and successful entry into the clinic, where safety and clinical efficacy of Ad.*mda*-7 (INGN 241) was confirmed in a Phase I clinical trial in patients with advanced carcinomas and melanomas (18–21). The most intriguing property of *mda*-7/IL-24 is preferential induction of apoptosis in cancer cells of diverse origin without harming normal cells (18–21). Additional attributes of *mda*-7/IL-24 that make it an ideal tool for cancer gene therapy include potent ''antitumor bystander'' activity, an ability to inhibit tumor angiogenesis, synergy with radiation, chemotherapy and monoclonal antibody therapies, and immunomodulatory activity (18–24).

Because of its wide range of biological effects and lack of toxicity in animal models, the effects of *mda*-7/IL-24 were examined in the present study to determine its ability to modulate MDR in P-gp–expressing human colorectal SW620/Dox cells. We show that *mda*-7/IL-24 down-regulates P-gp expression and reduces P-gp–mediated efflux in doxorubicin-resistant SW620/Dox cells. Our results also indicate that SW620/Dox cells are more sensitive to *mda*-7/IL-24–induced apoptosis induction than parental SW620 cells. Mechanistic analysis establishes that SW620/Dox cells exhibit increased basal reactive oxygen species (ROS) production and lower basal mitochondrial transmembrane potential than their drug-sensitive parental cells, and *mda*-7/IL-24 further ameliorates these properties resulting in preferential apoptosis in drug-resistant cells. These exciting findings indicate that *mda*-7/IL-24 might be a potent nontoxic therapeutic for reversal of drug resistance, providing a new strategy for effectively treating patients failing chemotherapy as a consequence of typical MDR.

Materials and Methods

Cell Culture and Reagents

The human SW620 colorectal carcinoma cell line was obtained from the American Type Culture Collection and cultured in RPMI 1640 (Life Technologies, Inc.) supplemented with 10% fetal bovine serum and 1% penicillin and streptomycin (Life Technologies) at 37°C in a 5% CO_2, 95% air humidified incubator. The human SW620/Dox colorectal carcinoma cell line was kindly provided by Dr. Myles Cabot (John Wayne Cancer Institute at Saint John's Health Center, Santa Monica, CA). Drug-sensitive (KB 3.1) and MDR drug-resistant (KB 3.1/Adr) human cervical carcinoma cell lines were provided by Dr. Michael M. Gottesman (National Cancer Institute, Bethesda, MD). The drug-resistant cells were grown in the presence of 1 μmol/L doxorubicin, which was withdrawn for two generations before doing experiments.

Recombinant Adenovirus Constructs

The recombinant replication-incompetent Ad.*mda*-7 was created in two steps as described previously and plaque purified by standard procedures (25).

3-(4,5-Dimethylthiazol-2-yl)-2,5-Diphenyltetrazolium Bromide Viability Assays

Viability assays were done as described previously (26). Briefly, cells were seeded in 96-well tissue culture plates (2×10^3 per well) and treated with different concentrations of doxorubicin or infected the next day with different adenoviruses. At the indicated time points, the medium was removed, and fresh medium containing 0.5 mg/mL 3-(4,5-dimethylthiazol-2-yl)-2,5-diphenyltetrazolium bromide was added to each well. The cells were incubated at 37°C for 4 h and then an equal volume of solubilization solution (0.01 N HCl in 10% SDS) was added to each well and mixed thoroughly. The absorbance from the plates was read on a Bio-Rad microplate reader model 550 at 595 nm. A statistical analysis of the results was done using the Analysis ToolPack provided by Microsoft Excel. A Student's two-sample *t* test, assuming unequal variances, was used to determine the equality of the means of two samples. The confidence level (α) was 0.05.

Transfection Assays with Small Interfering RNA

The control and *MDR* small interfering RNAs (siRNA) were purchased from Santa Cruz Biotechnology. Cells were transiently transfected with the control and *MDR* siRNAs according to the manufacturer's instructions.

Apoptosis Assay (Annexin V – Binding Assay)

Cells were trypsinized and washed once with complete medium. Aliquots of cells (5×10^5) were resuspended in complete medium (0.5 mL) and stained with allophycocyanin-labeled Annexin V (BD Biosciences) according to the manufacturer's instructions. 4′,6-Diamidino-2-phenylindole/propidium iodide was added to the samples after staining with Annexin V to exclude late apoptotic and necrotic cells. Flow cytometry was done immediately after staining.

Preparation of Cell Extracts and Western Blotting Analysis

Protein lysates were prepared on ice in a radioimmunoprecipitation assay buffer [50 mmol/L Tris-HCl (pH 8.0),

150 mmol/L NaCl, 0.1% SDS, 1% NP40, 0.5% sodium deoxycholate] with freshly added 0.1 mg/mL phenylmethylsulfonyl fluoride, 1 mmol/L sodium orthovanadate, and 1 mg/mL aprotinin. Protein concentrations were determined using the Bio-Rad protein assay system (Bio-Rad Laboratories). Aliquots of cell extracts containing 50 μg of total protein were resolved in 8% to 12% SDS-polyacrylamide gel and transferred to 0.45-μm nitrocellulose membranes (Osmonics). Filters were blotted using anti-EF-1α monoclonal (Upstate Cell Signaling), anti-P-gp monoclonal (Calbiochem), anti-rabbit MDA-7/IL-24, and anti-poly(ADP-ribose) polymerase (PARP) polyclonal (Cell Signaling Technology) antibodies. Enhanced chemiluminescence was done according to the manufacturer's recommendation.

Doxorubicin Accumulation and Efflux Assay

Doxorubicin accumulation and efflux were analyzed by flow cytometry (27, 28). The intracellular accumulation of doxorubicin was determined after SW620 and SW620/Dox cells were infected with either Ad.*vec* or Ad.*mda-7* (25 plaque-forming units/cell) for 24 h and then incubated with 2 and 4 μmol/L doxorubicin at 37°C for 60 min. After incubation, the cells were washed twice with ice-cold PBS, resuspended in 400 μL PBS, and then analyzed by flow cytometry. In doxorubicin efflux studies, cells were infected with either Ad.*vec* or Ad.*mda-7* at the indicated multiplicity of infection (MOI). At 24 h after infection, cells were incubated with 5 μmol/L doxorubicin for 30 min (substrate loading phase), washed twice with PBS, and incubated with drug-free medium for 45 min. After incubation, the cells were harvested, centrifuged, and washed in ice-cold PBS. Cell pellets were then resuspended in 400 μL PBS and used immediately for flow cytometric analysis for intracellular doxorubicin retention.

Anchorage-Independent Growth Assay

Cells were transiently transfected with either empty vector (pCDNA3.1) or *MDR1* and then infected with either Ad.*vec* or Ad.*mda-7* with the indicated MOI. Twenty-four hours later, cells (1×10^5) were replated in 0.4% Noble agar on 0.8% base agar. Two weeks later, colonies >50 cells were counted under a dissection microscope. Data represent mean ± SD of triplicate plates in three independent experiments.

Detection of Coxsackie-Adenovirus Receptors on the Cell Surface

Coxsackie-adenovirus receptors were determined as described previously (29). Two methods were used for semiquantitation of the results. The shift of FL1 peak was calculated as difference in peak channels between the controls (cells unstained or stained with nonspecific antibody) and the experimental cells stained with anti-Coxsackie-adenovirus receptor antibody relative to the position of the control cell peak channel. The second method uses the Kolmogorov-Smirnov test for overlaid histograms. The calculation computes the summation of the overlaid curves and determines the greatest difference between the summation curves (Kolmogorov-Smirnov statistics).

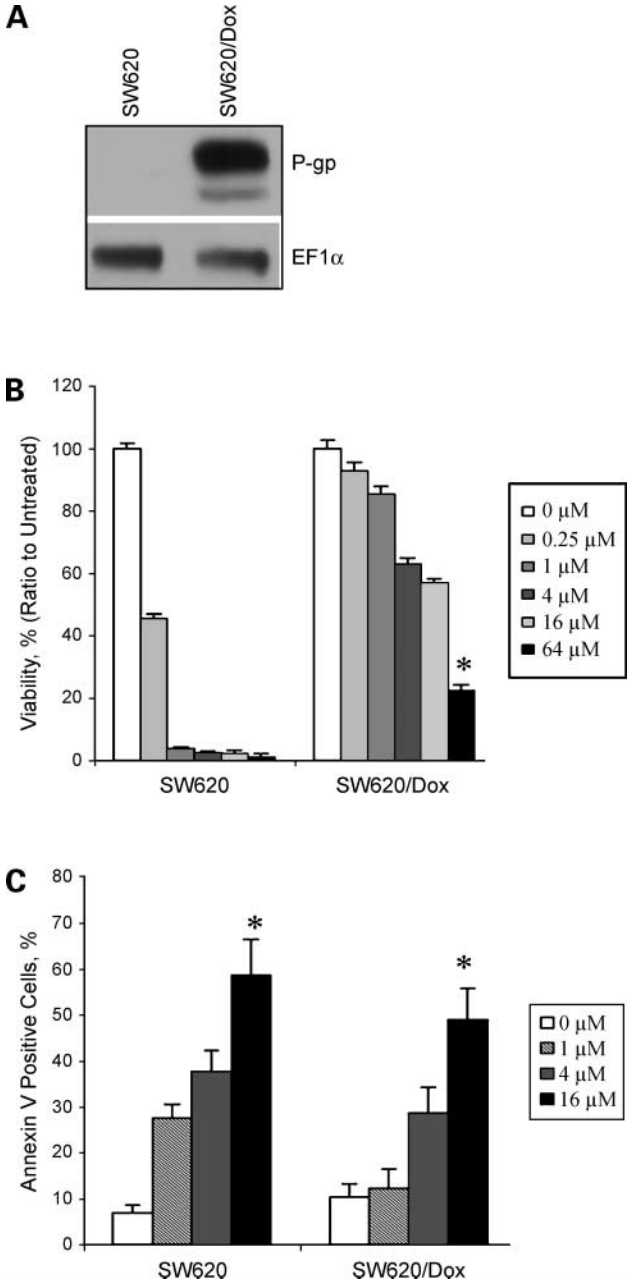

Figure 1. The SW620/Dox cell line is resistant to doxorubicin and overexpresses P-gp. **A,** Western blot analysis of endogenous P-gp levels in SW620 and SW620/Dox cells. **B,** effect of different doses of doxorubicin on cell growth in SW620 and SW620/Dox cells. Cells were cultured in the presence of different concentrations of doxorubicin (0.25, 1, 4, 16, and 64 μmol/L) for 5 d. The effects on cell viability were determined by 3-(4,5-dimethylthiazol-2-yl)-2,5-diphenyltetrazolium bromide assay. *Columns,* average of results of three independent experiments; *bars,* SD. Statistical significance was determined by Student's *t* test. *, $P < 0.05$. **C,** effect of doxorubicin on apoptosis induction in SW620 and SW620/Dox cells by Annexin V–binding assay. Cells were treated with the various concentrations of doxorubicin as shown in **B** and stained 48 h after treatment with allophycocyanin-labeled Annexin V. The percentage of early and late apoptotic cells (only Annexin V stained) was calculated using FlowJo version 6.31 software. *Columns,* average of replicate studies; *bars,* SD. Statistical significance was determined by Student's *t* test. *, $P < 0.05$.

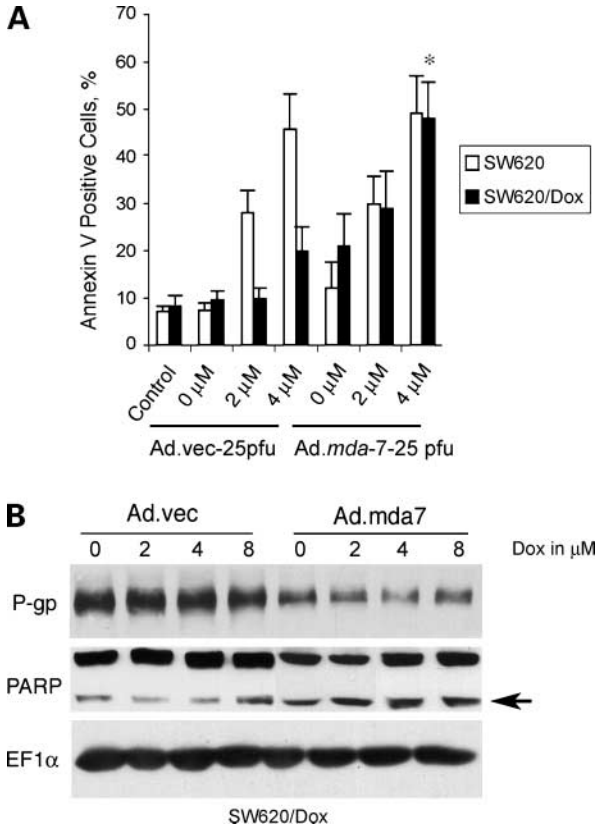

Figure 2. Ad.*mda*-7 infection induces MDR reversal in SW620/Dox cells. **A,** SW620 and SW620/Dox cells were infected with either Ad.*vec* or Ad.*mda*-7 [25 plaque-forming units (*pfu*)/cell] and then treated with the indicated concentrations of doxorubicin for 48 h. The percentage of apoptotic cells was determined by Annexin V–binding assay and flow cytometry. Statistical significance was determined by Student's *t* test. *, $P < 0.05$ in Ad.*mda*-7 + 4 mol/L doxorubicin–treated SW620/Dox cells compared with Ad.*vec* + 4 mol/L doxorubicin–treated SW620/Dox cells. **B,** Ad.*mda*-7 infection down-regulates P-gp expression and induces PARP cleavage in SW620/Dox cells. Cells were infected with either Ad.*vec* or Ad.*mda*-7 (25 plaque-forming units/cell) and then treated with the indicated concentrations of doxorubicin (*Dox*) for 24 h. Total proteins were extracted and Western blot analysis was done with the indicated antibodies. *Arrow,* cleaved product of PARP.

Assessment of Mitochondrial $\Delta\psi_\mu$ and ROS Production

Changes in mitochondrial transmembrane potential $\Delta\psi_\mu$ were determined by staining cells in 20 nmol/L $DiOC_6$ in PBS for 30 min at 37°C in the dark (30). The dye accumulates in actively respiring mitochondria depending on $\Delta\psi_\mu$. To determine ROS production, cells were stained with 5 μmol/L DCFH-DA in PBS for 30 min at 37°C in the dark (30). Immediately after staining, cells were analyzed by flow cytometry (FACScan, Becton Dickinson), and data were analyzed using CellQuest software version 3.1 (Becton Dickinson).

Statistical Analysis

All the experiments were done at least thrice. The results are expressed as mean ± SE. Statistical comparisons were made using an unpaired two-tailed Student's *t* test. A *P* value of <0.05 was considered to be significant.

Results

SW620/Dox Cells Overexpress P-gp and Display Resistance to Doxorubicin

We first characterized the MDR colorectal carcinoma SW620/Dox cell line and its drug-sensitive parental line SW620 for their sensitivity to doxorubicin and expression of transporter molecules. Western blot analysis with a monoclonal anti-P-gp antibody confirmed that SW620/Dox cells expressed elevated levels of P-gp (Fig. 1A) with barely detectable levels of P-gp in parental SW620 cells. Doxorubicin (a known P-gp substrate) was used to characterize the drug-resistant phenotype. In accordance with P-gp expression, the SW620/Dox cells were 100 times more resistant to doxorubicin than SW620 cells as assessed by cell viability assay 5 days after doxorubicin treatment (Fig. 1B). Whereas the IC_{50} of doxorubicin for SW620 cells was 0.25 μmol/L, for SW620/Dox cells it was 25 μmol/L. More importantly, 1 μmol/L and higher doses of doxorubicin reduced viability of SW620 cells by >95%, whereas in SW620/Dox cells >50% of cells were viable even with 16 μmol/L doxorubicin, and with 64 μmol/L of the drug ~20% of cells were still viable. Results of apoptosis analysis by Annexin V–binding assay 48 h after doxorubicin treatment confirmed the resistant phenotype of SW620/Dox cells (Fig. 1C). Whereas 1 μmol/L doxorubicin treatment induced apoptosis in ~25% of SW620 cells, only ~10% of SW620/Dox cells were apoptotic, which was similar to control untreated cells. At higher doses, apoptosis induction in both SW620 and SW620/Dox cells was comparable, which might be attributed to the assay being done at an earlier time point (48 h).

Resistance of SW620/Dox Cells to Doxorubicin Is Reversed by *mda*-7/IL-24

Next, we explored the growth-inhibitory effect of *mda*-7/IL-24 on SW620 and SW620/Dox cells. We delivered *mda*-7/IL-24 by means of a replication-incompetent adenovirus (Ad.*mda*-7) and an empty adenovirus (Ad.*vec*) that served as a control. Cells were infected with either Ad.*vec* or Ad.*mda*-7 and incubated with doxorubicin (2 and 4 μmol/L) and Annexin V–binding assays were done to evaluate apoptosis induction. An enhancement of sensitivity to doxorubicin was observed when SW620/Dox cells were infected with Ad.*mda*-7 (Fig. 2A). Whereas ~10% and ~20% of apoptotic cells were detected with Ad.*vec* + 2 μmol/L doxorubicin and Ad.*vec* + 4 μmol/L doxorubicin treatment, respectively, ~30% and ~50% of apoptotic cells were detected with Ad.*mda*-7 + 2 μmol/L doxorubicin and Ad.*mda*-7 + 4 μmol/L doxorubicin treatment, respectively. Intriguingly, the cytotoxic effect of doxorubicin in the SW620 cell line was not significantly altered by Ad.*mda*-7 infection. Comparable results were obtained with another variant of drug-sensitive and drug-resistant human cervical carcinoma cells (KB 3.1 and KB 3.1/Adr; Supplementary Fig. S2A).[6] The increase in apoptotic potential of SW620/

[6] Supplementary material for this article is available at Molecular Cancer Therapeutics Online (http://mct.aacrjournals.org/).

Dox cells to doxorubicin following Ad.*mda*-7 infection was confirmed by the appearance of PARP cleavage, a marker of apoptosis induction (Fig. 2B). Cleaved PARP could only be detected with Ad.*vec* + 8 μmol/L doxorubicin, whereas Ad.*mda*-7 alone could induce PARP cleavage, which was further augmented by as little as 2 μmol/L doxorubicin. We also determined the level of expression of P-gp protein in Ad.*vec*-treated and Ad.*mda*-7–treated SW620/Dox cells by Western blot analysis and immunofluorescence microscopy. As shown in Fig. 2B and Supplementary Fig. S1,[6] *mda*-7/IL-24 modestly decreased P-gp protein in SW620/Dox cells, indicating that down-regulation of P-gp might be a potential mechanism of reversal of the MDR phenotype following Ad.*mda*-7 infection.

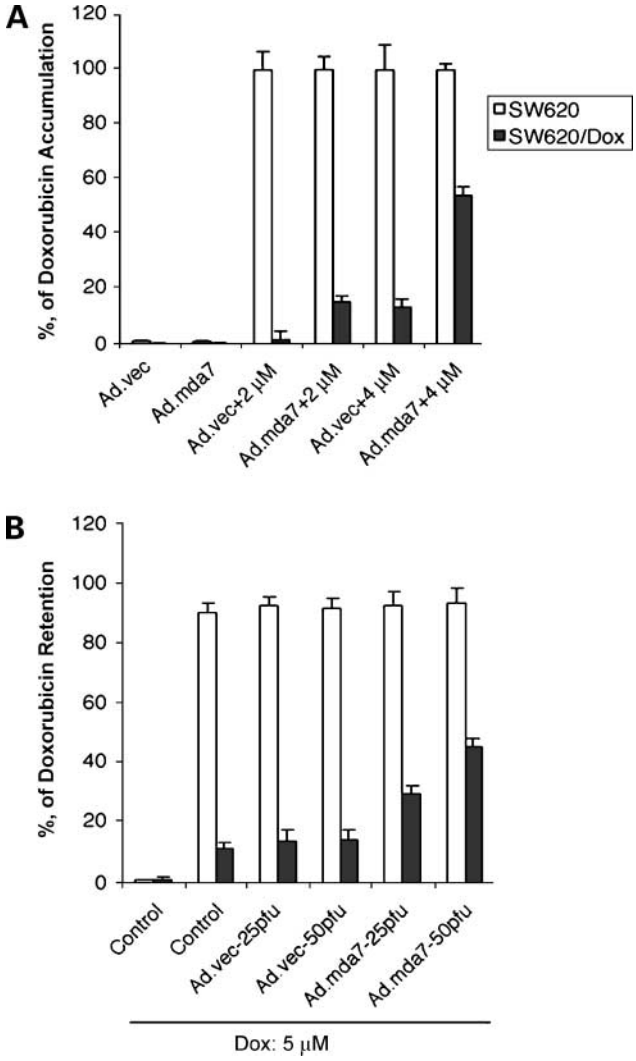

Figure 3. Effect of Ad.*mda*-7 on the accumulation and efflux of doxorubicin in SW620 and SW620/Dox cells. **A,** the intracellular accumulation of doxorubicin was determined after cells were infected with either Ad.*vec* or Ad.*mda*-7 (25 plaque-forming units/cell) for 24 h and then incubated with 2 and 4 μmol/L of doxorubicin for 60 min. After incubation, the cells were washed twice with ice-cold PBS, resuspended in 400 μL PBS, and then analyzed by flow cytometry. Bar graphical presentation of doxorubicin accumulation. *Columns,* average of three independent experiments; *bars,* SD. **B,** for doxorubicin efflux assays, cells were infected with either Ad.*vec* or Ad.*mda*-7 at the indicated MOI. At 24 h after infection, cells were incubated with 5 μmol/L doxorubicin for 30 min (substrate loading phase), washed twice with PBS, and incubated with drug-free medium for 45 min. After incubation, the cells were harvested, centrifuged, and washed in ice-cold PBS. Cell pellets were then resuspended in 400 μL PBS and used immediately for flow cytometric analysis for intracellular doxorubicin retention. Bar graphical presentation of doxorubicin retention. *Columns,* average of three independent experiments; *bars,* SD.

Effect of *mda*-7/IL-24 on Doxorubicin Accumulation and Efflux

P-gp causes efflux of chemotherapeutic drug from cells (31, 32). To examine the effect of *mda*-7/IL-24 on P-gp function on the surface of viable cells, doxorubicin accumulation and efflux studies were done by flow cytometry as sensitive indicators of P-gp activity (28, 33). As shown in Fig. 3A, doxorubicin accumulation in Ad.*vec*-infected SW620 cells was markedly higher than Ad.*vec*-infected SW620/Dox cells and Ad.*mda*-7 infection did not augment this accumulation further in SW620 cells. However, a significant increase in intracellular doxorubicin accumulation was evident in SW620/Dox cells following Ad.*mda*-7 infection. With 4 μmol/L doxorubicin, accumulation increased from ~15% in Ad.*vec*-infected SW620/Dox cells to ~50% in Ad.*mda*-7–infected cells. Essentially similar results were obtained with another variant of drug-sensitive and drug-resistant cells (KB 3.1 and KB 3.1/Adr; Supplementary Fig. S2B).[6] The efflux of doxorubicin from SW620 and SW620/Dox cells was also detected by flow cytometry. The cells were either uninfected or infected with Ad.*vec* or Ad.*mda*-7 for 24 h (Fig. 3B) and incubated with 5 μmol/L doxorubicin at 37°C for 30 min as described in Materials and Methods. The levels of doxorubicin efflux in SW620/Dox cells were significantly higher than that in SW620 cells after infection with Ad.*vec*. Ad.*mda*-7 infection caused a significant decrease (~3-fold when compared with control) in the amount of doxorubicin effluxed in SW620/Dox cells but had no effect in SW620 cells. Taken together, these results imply that *mda*-7/IL-24 treatment induced MDR reversal in drug-resistant cells by inhibiting P-gp function (as evidenced by decreased P-gp level, increased intracellular doxorubicin accumulation, and decreased efflux of doxorubicin), which leads to an accumulation of doxorubicin enabling it to exert its cytotoxic effects.

Ad.*mda*-7 Induces Preferential Growth Inhibition and Apoptosis of P-gp–Overexpressing SW620/Dox Cells

Our initial Annexin V–binding assays in drug-sensitive and drug-resistant cell lines indicated that Ad.*mda*-7 induced more apoptotic death in SW620/Dox cells (~20%) than in SW620 cells (~10%; Fig. 2A), which prompted us to further pursue this phenomena in detail. The results presented in Fig. 4A revealed that, in 3-(4,5-dimethylthiazol-2-yl)-2,5-diphenyltetrazolium bromide assays, Ad.*mda*-7 reduced the viability of SW620/Dox cells in a dose-dependent manner with no significant viability change in SW620 cells that was consistent with our previous report (34). We also investigated the effects of

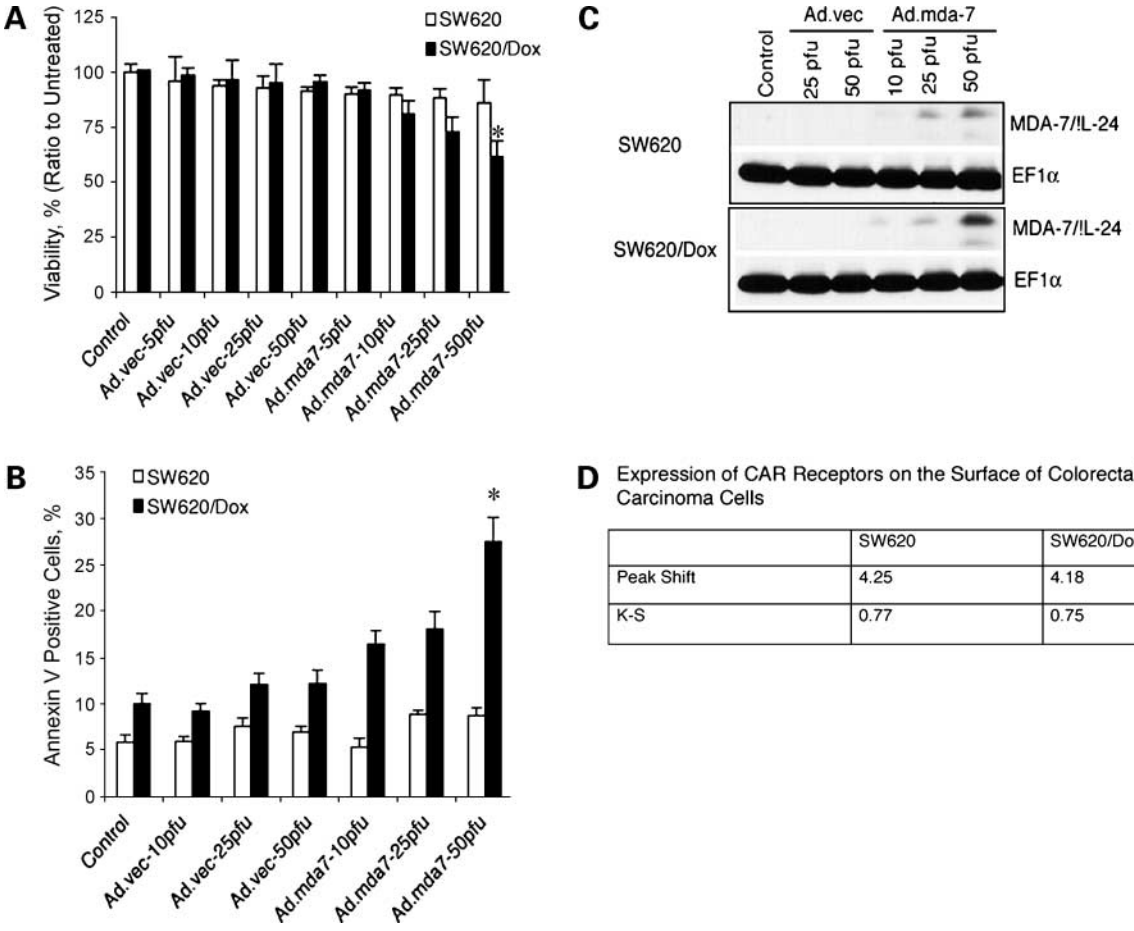

D Expression of CAR Receptors on the Surface of Colorectal Carcinoma Cells

	SW620	SW620/Dox
Peak Shift	4.25	4.18
K-S	0.77	0.75

Figure 4. Ad.*mda*-7 inhibits cell growth and induces apoptosis preferentially in P-gp–overexpressing MDR variant SW620/Dox cells. **A,** SW620 and SW620/Dox cells were infected with either Ad.*vec* or Ad.*mda*-7 with the indicated MOI and cell viability was determined by 3-(4,5-dimethylthiazol-2-yl)-2,5-diphenyltetrazolium bromide assay at 5 d after infection. *Columns,* average of three independent experiments; *bars,* SD. Statistical significance was determined by Student's *t* test. *, $P < 0.05$. **B,** effect of Ad.*mda*-7 infection on apoptosis induction in SW620 and SW620/Dox cells by Annexin V–binding assay. Cells were infected as indicated in **A** and stained after 48 h with allophycocyanin-labeled Annexin V and immediately analyzed by flow cytometry. The percentage of early and late apoptotic cells (only Annexin V stained) was calculated using FlowJo version 6.31 software. Statistical significance was determined by Student's *t* test. *, $P < 0.05$. **C,** MDA-7/IL-24 protein expression in SW620 and SW620/Dox cells following infection with Ad.*mda*-7 determined by Western blot analysis. **D,** analysis of Coxsackie-adenovirus receptor (*CAR*) expression level in SW620 and SW620/Dox cells. *K-S,* Kolmogorov-Smirnov.

mda-7/IL-24 on apoptosis induction using Annexin V–binding assays, the results of which confirmed the viability assays (Fig. 4B). With Ad.*mda*-7 infection at 50 plaque-forming units/cell, ~10% of SW620 and ~25% of SW620/Dox cells were apoptotic. We checked the level of MDA-7/IL-24 protein following Ad.*mda*-7 infection in these two cell lines. Interestingly, SW620/Dox cells expressed more MDA-7/IL-24 protein than SW620 cells following infection with Ad.*mda*-7 (Fig. 4C) despite a comparable level of Coxsackie-adenovirus receptors necessary for adenovirus transduction (Fig. 4D).

Overexpression of *MDR1* Renders SW620 Cells More Sensitive to Ad.*mda*-7–Induced Apoptosis

To determine if a direct causal relationship exists between overexpression of *MDR1*, which encodes P-gp, and increased sensitivity to *mda*-7/IL-24–induced apoptosis, we transiently transfected *MDR1* into SW620 cells and did Annexin V–binding assays for apoptosis detection. As shown in Fig. 5A, infection with Ad.*mda*-7 significantly increased apoptotic induction in *MDR1*-transfected SW620 cells, whereas no significant difference was evident in empty vector (pcDNA3.1)-transfected cells. Interestingly, transfection of *MDR1* in SW620 cells resulted in generation of more MDA-7/IL-24 protein than that observed in empty vector–transfected cells following Ad.*mda*-7 infection (Fig. 5B). We also investigated the effects of *MDR1* and Ad.*mda*-7 on long-term anchorage-independent cell growth by determining colony-forming ability in soft agar. The cloning efficiency of SW620 cells was significantly decreased with *MDR1* transfection and Ad.*mda*-7 infection when compared with either agent alone (Fig. 5C). These results further substantiate the direct correlation between overexpression of *MDR1* and *mda*-7/IL-24–induced enhanced growth inhibition.

siRNA Knockdown of *MDR1* Partially Protects SW620/Dox Cells from *mda*-7/IL-24–Induced Apoptosis

To provide further evidence that *MDR1*/P-gp plays a major role in the enhanced *mda*-7/IL-24 sensitivity of SW620/Dox drug-resistant cells, we used a siRNA approach to knock down the expression of *MDR1*. For this experiment, cells were transiently transfected with *MDR1* siRNA or control siRNA and then infected with either

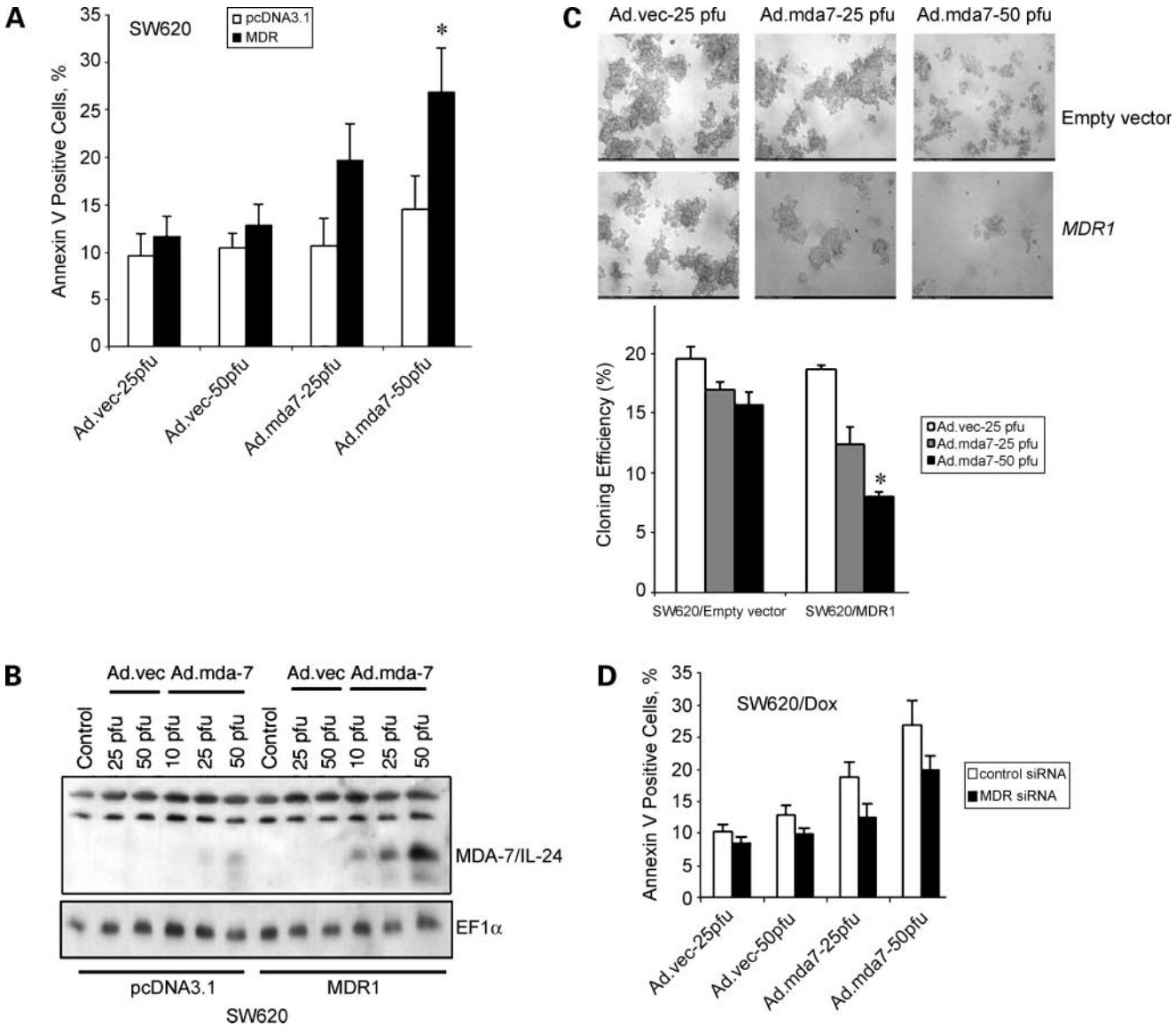

Figure 5. Overexpression of *MDR1* induces increased sensitivity to Ad.*mda*-7 infection in SW620 cells and down-regulation of MDR partially protects SW620/Dox cells from Ad.*mda*-7–induced apoptosis. **A,** SW620 cells were transiently transfected with either empty vector (pcDNA3.1) or *MDR1* and then infected with either Ad.*vec* or Ad.*mda*-7 at the indicated MOIs. Apoptosis induction was evaluated by Annexin V–binding assay 48 h after infection. The percentage of early and late apoptotic cells (only Annexin V stained) was calculated using FlowJo version 6.31 software. Statistical significance was determined by Student's *t* test. *, $P < 0.05$. **B,** effect of *MDR1* overexpression on MDA-7/IL-24 protein expression. Western blot analysis was done with SW620 cell lysates harvested at 24 h after infection. **C,** ectopic expression of *MDR1* in SW620 cells significantly inhibits colony formation in soft agar following infection with Ad.*mda*-7. Cells were transiently transfected with either empty vector (pcDNA3.1) or *MDR1* and then infected with either Ad.*vec* or Ad.*mda*-7 with the indicated MOI. Twenty-four hours later, cells (1×10^5) were replated in 0.4% agar on 0.8% base agar. Two weeks later, colonies >50 cells were counted under a dissection microscope. *Top,* photomicrographs of soft agar plate; *bottom,* graphical representation of the soft agar assays. *Columns,* mean of three independent experiments; *bars,* SD. Statistical significance was determined by Student's *t* test. *, $P < 0.05$. **D,** SW620/Dox cells were transiently transfected with either control siRNA or *MDR1* siRNA using Lipofectamine before infection with either Ad.*vec* or Ad.*mda*-7 at the indicated MOI. Forty-eight hours later, apoptosis was measured by Annexin V–binding assay using allophycocyanin-conjugated Annexin V by flow cytometry. The percentage of early and late apoptotic cells (only Annexin V stained) was calculated using FlowJo version 6.31 software.

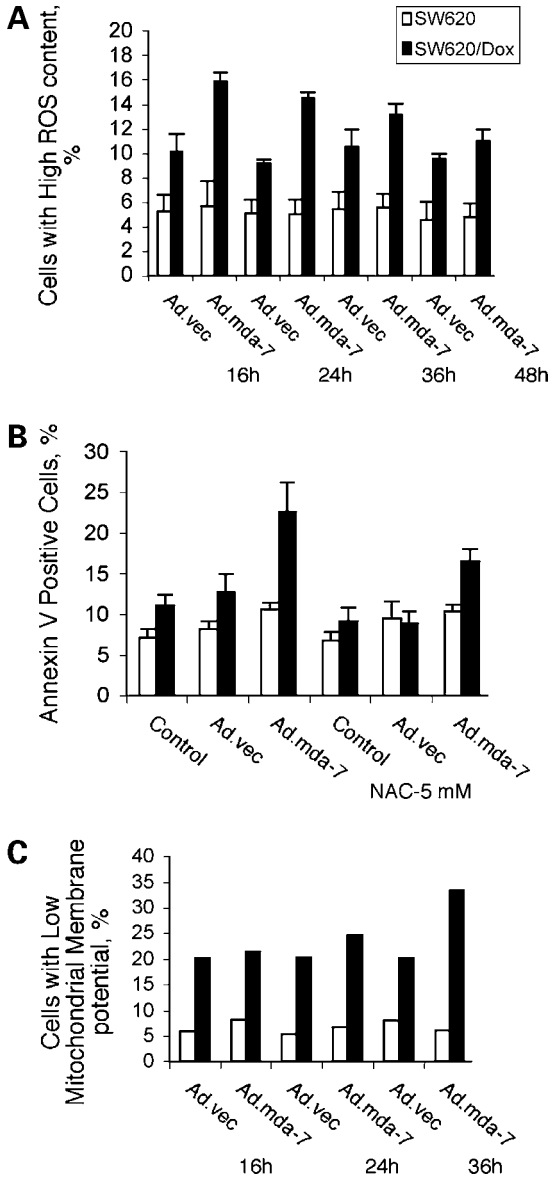

Figure 6. Kinetics of ROS generation, apoptosis induction, and mitochondrial alteration induced by Ad.*mda*-7 in drug-sensitive and drug-resistant cells. Cells were infected with Ad.*vec* or Ad.*mda*-7 and analyzed by flow cytometry at indicated times. **A,** ROS generation was measured using DCFH-DA. **B,** apoptotic changes were detected by Annexin V–binding assay at 36 h after infection. **C,** changes in the mitochondrial transmembrane potential $\Delta\psi_\mu$ were measured with $DiOC_6$. *Columns,* average of three independent experiments; *bars,* SD.

Ad.*vec* or Ad.*mda*-7. Apoptosis induction was analyzed at 48 h after infection by Annexin V–binding assays. As shown in Fig. 5D, cells treated with *MDR1* siRNA reduced the sensitivity of SW620/Dox cells to *mda*-7/IL-24 ~1.5-fold relative to cells transfected with control siRNA, indicating a direct association between *MDR1* overexpression and *mda*-7/IL-24 sensitivity. Analogous results were obtained after a 3-h preincubation with 20 μg/mL of anti-P-gp monoclonal antibody, known to inhibit P-gp function (data not shown).

Ad.*mda*-7 Selectively Induces ROS Production and a $\Delta\psi_\mu$ Reduction in SW620/Dox Drug-Resistant Cells

ROS regulates apoptosis and proliferation in response to a variety of stimuli, including tumor necrosis factor-α, UV and γ-irradiation, and anthracyclines (35). Previous studies document that ROS contributes to the ability of *mda*-7/IL-24 to synergize with radiation to kill renal carcinoma cells, and it plays a significant role in the ability of Ad.*mda*-7 to induce apoptosis selectively in prostate cancer cells (30, 36). Additionally, several studies have shown that drug-resistant cells possessed a more active mitochondrial electron transport chain than their parental cell lines and were more susceptible to a variety of stress stimuli. Based on these considerations, we determined ROS and $\Delta\psi_m$ (two important variables for mitochondrial integrity) in Ad.*vec*-treated and Ad.*mda*-7–treated drug-sensitive and drug-resistant cells. Interestingly, flow cytometry analysis of cellular fluorescence revealed that SW620/Dox cells showed more basal ROS generation and reduced $\Delta\psi_m$ than SW620 cells (Fig. 6). Ad.*mda*-7 infection produced a further increase in ROS production in SW620/Dox cells but not in SW620 cells (Fig. 6A), which was apparent at 16 and 24 h following Ad.*mda*-7 infection. The increase in ROS production coincided with apoptosis induction in the SW620/Dox cells, as confirmed by Annexin V–binding assays (Fig. 6B). In the presence of noncytotoxic doses of a general antioxidant, NAC (5 mmol/L), the apoptosis-inducing activity of Ad.*mda*-7 was abrogated in SW620/Dox cells (Fig. 6B). These observations suggest that free radicals may contribute to Ad.*mda*-7 induction of apoptosis in drug-resistant cells. Because ROS is a modulator of mitochondrial membrane potential loss, we determined the time course of mitochondrial changes by measuring $\Delta\psi_m$. Cells were infected with Ad.*vec* or Ad.*mda*-7, collected at different times up to 36 h, and stained with the cationic mitochondrial dye $DiOC_6$, which accumulates in active mitochondria, to determine changes in $\Delta\psi_m$ (30). As shown in Fig. 6C, the decline in $\Delta\psi_m$ and the increase in Annexin V–binding assays occurred concomitantly, consistent with prior reports of apoptosis-associated events in other cell types (37). These studies provide mechanistic insight that preferential induction of apoptosis in MDR-overexpressed SW620/Dox cells by Ad.*mda*-7 is linked to changes in mitochondrial function (reduction in $\Delta\psi_m$) and ROS generation.

Discussion

Chemotherapy is the most frequent treatment for patients who suffer from metastatic cancers. The effectiveness of chemotherapy, however, is seriously limited by MDR that is mainly due to the overexpression of P-gp, a pump protein crucially involved in drug transport from the inside to the outside of cancer cells, preventing the intracellular accumulation of anticancer drugs inside cancer cells necessary for cytotoxic activity. Accordingly, novel agents that can inhibit the drug transporter function of P-gp or its

expression have the potential to overcome the MDR phenotype by enhancing intracellular accumulation of anticancer drugs.

Gene therapy provides a viable option, especially when used with a cancer-selective apoptosis-inducing gene, such as *mda-7/IL-24*, which induces a direct antitumor effect and profound antitumor ''bystander'' activity. The present study illustrates that treatment with *mda*-7/IL-24 can lead to a reversal of the MDR phenotype by inhibiting P-gp function, which allows for the intracellular accumulation of anticancer drugs. Our data show that *mda*-7/IL-24 is very potent at reversing the accumulation deficit and at blocking the efflux of P-gp substrate doxorubicin from the P-gp–overexpressing cell lines SW620/Dox (Fig. 3). The finding that drug efflux and accumulation were not affected in the SW620 parental cells (P-gp nonexpressing) strongly indicates that the reversal of drug resistance by *mda*-7/IL-24 is probably attributable to the inhibition of P-gp–mediated efflux. Additionally, the increased accumulation of anticancer drugs in response to *mda*-7/IL-24 dramatically enhances apoptotic potential, as evidenced by the observations that cotreatment with Ad.*mda*-7 increases apoptosis (Annexin V–binding assay) and PARP cleavage by doxorubicin (Fig. 2A and B) in drug-resistant cells. Analogous results were obtained with other variants of extrinsic and intrinsic MDR cells (KB 3.1/Adr and HCT15 cells; Supplementary Fig. S2;[6] data not shown). Overall, our data document for the first time that MDR reversal by *mda*-7/IL-24 is a common property shared among extrinsic and intrinsic MDR human cancer cell lines that overexpress P-gp compared with their parental, drug-sensitive counterparts. Our results also provide preliminary evidence for the applicability of *mda*-7/IL-24 to other tumor types, such as leukemia, sarcoma, and adrenocortical cancers, which intrinsically express P-gp. In contrast, normal human renal epithelial cells and rat hepatocytes that are reported to display enhanced P-gp expression were not sensitive to *mda*-7/IL-24 treatment (data not shown; ref. 36), supporting the differential activity of this novel cytokine for cancer therapy. For several tumor types, the precise contribution of P-gp to drug resistance has been difficult to quantify because these tumors are often resistant to both *MDR1* substrates and nonsubstrates. Further experiments are required to determine if drug and *mda*-7/IL-24 sensitivity also extends to these diverse tumor types.

Of particular relevance for cancer therapy is the finding that MDR-expressing tumor cells were much more sensitive to the cytotoxic effect of *mda*-7/IL-24 than their parental tumor counterparts. A similar enhanced sensitivity to different stress agents, such as tumor necrosis factor–related apoptosis-inducing ligand, spermine, and NSC 73306, was shown in several drug-resistant cells when compared with parental cells (33, 38, 39). Additionally, human small cell lung carcinoma cell lines showed a collateral sensitivity to 2′,2′-difluorodeoxycytidine (gemcitabine) and 1-β-D-arabinofuranosylcytosine. H69/DAU, a daunorubicin-resistant variant of H69 with a P-gp overexpression, and NYH/VM, a VM-26 (teniposide)-resistant variant of NYH with an at-MDR, were both 2-fold more sensitive to gemcitabine and 7- and 2-fold more sensitive to 1-β-D-arabinofuranosylcytosine, respectively (40). Using gain-of-function (overexpression) and loss-of-expression (knockdown) experiments, we confirmed our initial observations that *mda*-7/IL-24 preferentially induced apoptosis in *MDR1*/P-gp–overexpressing cells (Fig. 5). Interestingly, we observed more MDA-7/IL-24 proteins in *MDR1*-transfected cell lysates than that in empty vector–transfected cell lysates following Ad.*mda*-7 infection (Fig. 5B); the mechanism(s) underlying this phenomenon is not known. Moreover, we elucidate the potential mechanisms of enhanced *mda*-7/IL-24–induced apoptosis in drug-resistant cells. Specifically, our analysis indicates that the enhancement of *mda*-7/IL-24–mediated apoptosis in P-gp–overexpressing SW620/Dox cells was associated with increased ROS production and lower $\Delta\psi_m$. Differences in mitochondrial electron transport chain activity between sensitive and resistant cell lines have been reported. In particular, Jia et al. (41) showed that the daunorubicin-resistant subline K/DAU600 and the vinblastine-resistant cell line CEM/VBL100, which highly expressed P-gp, possessed a more active mitochondrial electron transport chain than their parental K562 and CCRF-CEM cell lines. Furthermore, drug-resistant cells with increased activity of the respiratory chain were more susceptible to tumor necrosis factor-α–induced, etoposide-induced, and cytarabine-induced apoptosis than their parental counterparts (41, 42). Therefore, SW620/Dox cells may be more sensitive to *mda*-7/IL-24 because of their higher mitochondrial electron transport chain activity. Indeed, our results confirmed that SW620/Dox cells possessed more basal ROS and lower $\Delta\psi_m$ than their parental cells. When SW620/Dox cells were further treated with Ad.*mda*-7, a known ROS inducer (30, 36), the cells were no longer able to remove additional ROS and underwent a loss of mitochondrial functionality earlier and to a greater extent than SW620 cells, resulting in the induction of apoptosis. This conclusion is strengthened by the observations that pretreatment with a noncytotoxic dose of NAC significantly protected the drug-resistant cells from Ad.*mda*-7–induced apoptosis (Fig. 6B). Decreased mitochondrial membrane potential has been described as an event occurring in apoptosis induced by a variety of agents, including *mda*-7/IL-24. Our results, therefore, postulate a direct correlation between increased *mda*-7/IL-24–mediated apoptosis induction in SW620/Dox cells and decreased $\Delta\psi_m$. This observation was supported by a recent report that treatment with small cell-permeable nonpeptide inhibitors of antiapoptotic protein Bcl-2 reduced $\Delta\psi_m$, generated ROS, increased mitochondrial respiration, and decreased ATP synthesis in CEM leukemia cells (43).

In conclusion, our results indicate that (*a*) *mda*-7/IL-24 is a potent MDR reversal agent and (*b*) *mda*-7/IL-24 preferentially induces apoptosis in P-gp–overexpressing cells with altered mitochondrial functionality, supporting the potential of *mda*-7/IL-24 as an attractive targeted and safe therapy for treating malignant tumors with P-gp–mediated MDR.

References

1. Gottesman MM. How cancer cells evade chemotherapy: sixteenth Richard and Hinda Rosenthal Foundation Award Lecture. Cancer Res 1993;53:747 – 54.

2. Ambudkar SV, Kimchi-Sarfaty C, Sauna ZE, Gottesman MM. P-glycoprotein: from genomics to mechanism. Oncogene 2003;22:7468 – 85.

3. Dean M, Rzhetsky A, Allikmets R. The human ATP-binding cassette (ABC) transporter superfamily. Genome Res 2001;11:1156 – 66.

4. Juliano RL, Ling V. A surface glycoprotein modulating drug permeability in Chinese hamster ovary cell mutants. Biochim Biophys Acta 1976; 455:152 – 62.

5. Ueda K, Cardarelli C, Gottesman MM, Pastan I. Expression of a full-length cDNA for the human ''MDR1'' gene confers resistance to colchicine, doxorubicin, and vinblastine. Proc Natl Acad Sci U S A 1987; 84:3004 – 8.

6. Gros P, Croop J, Housman D. Mammalian multidrug resistance gene: complete cDNA sequence indicates strong homology to bacterial transport proteins. Cell 1986;47:371 – 80.

7. Johnstone RW, Cretney E, Smyth MJ. P-glycoprotein protects leukemia cells against caspase-dependent, but not caspase-independent, cell death. Blood 1999;93:1075 – 85.

8. Choi KH, Chen CJ, Kriegler M, Roninson IB. An altered pattern of cross-resistance in multidrug-resistant human cells results from spontaneous mutations in the mdr1 (P-glycoprotein) gene. Cell 1988;53:519 – 29.

9. Safa AR. Photoaffinity labels for characterizing drug interaction sites of P-glycoprotein. Methods Enzymol 1998;292:289 – 307.

10. Scotto KW. Transcriptional regulation of ABC drug transporters. Oncogene 2003;22:7496 – 511.

11. Cano-Gauci DF, Riordan JR. Action of calcium antagonists on multidrug resistant cells. Specific cytotoxicity independent of increased cancer drug accumulation. Biochem Pharmacol 1987;36:2115 – 23.

12. Tan B, Piwnica-Worms D, Ratner L. Multidrug resistance transporters and modulation. Curr Opin Oncol 2000;12:450 – 8.

13. Sikic BI, Fisher GA, Lum BL, Halsey J, Beketic-Oreskovic L, Chen G. Modulation and prevention of multidrug resistance by inhibitors of P-glycoprotein. Cancer Chemother Pharmacol 1997;40 Suppl:S13 – 9.

14. Di Nicolantonio F, Knight LA, Glaysher S, et al. *Ex vivo* reversal of chemoresistance by tariquidar (XR9576). Anticancer Drugs 2004;15: 861 – 9.

15. Robert J, Jarry C. Multidrug resistance reversal agents. J Med Chem 2003;46:4805 – 17.

16. Jiang H, Lin JJ, Su ZZ, Goldstein NI, Fisher PB. Subtraction hybridization identifies a novel melanoma differentiation associated gene, *mda*-7, modulated during human melanoma differentiation, growth and progression. Oncogene 1995;11:2477 – 86.

17. Jiang H, Su ZZ, Lin JJ, Goldstein NI, Young CSH, Fisher PB. The melanoma differentiation associated gene *mda*-7 suppresses cancer cell growth. Proc Natl Acad Sci U S A 1996;93:9160 – 5.

18. Gupta P, Su ZZ, Lebedeva IV, et al. *mda*-7/IL-24: multifunctional cancer-specific apoptosis-inducing cytokine. Pharmacol Ther 2006;111: 596 – 628.

19. Fisher PB. Is *mda*-7/IL-24 a ''magic bullet'' for cancer? Cancer Res 2005;65:10128 – 38.

20. Lebedeva IV, Sauane M, Gopalkrishnan RV, et al. *mda*-7/IL-24: exploiting cancer's Achilles' heel. Mol Ther 2005;11:4 – 18.

21. Sarkar D, Lebedeva IV, Gupta P, et al. Melanoma differentiation associated gene-7 (*mda*-7)/IL-24: a 'magic bullet' for cancer therapy? Expert Opin Biol Ther 2007;7:577 – 86.

22. Ramesh R, Mhashilkar AM, Tanaka F, et al. Melanoma differentiation-associated gene 7/interleukin (IL)-24 is a novel ligand that regulates angiogenesis via the IL-22 receptor. Cancer Res 2003;63:5105 – 13.

23. Su ZZ, Lebedeva IV, Sarkar D, et al. Melanoma differentiation associated gene-7, *mda*-7/IL-24, selectively induces growth suppression, apoptosis and radiosensitization in malignant gliomas in a p53-independent manner. Oncogene 2003;22:1164 – 80.

24. Su Z, Emdad L, Sauane M, et al. Unique aspects of *mda*-7/IL-24 antitumor bystander activity: establishing a role for secretion of MDA-7/IL-24 protein by normal cells. Oncogene 2005;24:7552 – 66.

25. Su ZZ, Madireddi MT, Lin JJ, et al. The cancer growth suppressor gene *mda*-7 selectively induces apoptosis in human breast cancer cells and inhibits tumor growth in nude mice. Proc Natl Acad Sci U S A 1998; 95:14400 – 5.

26. Emdad L, Sarkar D, Lebedeva IV, et al. Ionizing radiation enhances adenoviral vector expressing *mda*-7/IL-24-mediated apoptosis in human ovarian cancer. J Cell Physiol 2006;208:298 – 306.

27. Lehnert M, de Giuli R, Twentyman PR. Sensitive and rapid bioassay for analysis of P-glycoprotein-inhibiting activity of chemosensitizers in patient serum. Clin Cancer Res 1996;2:403 – 10.

28. Zhu HJ, Wang JS, Guo QL, Jiang Y, Liu GQ. Reversal of P-glycoprotein mediated multidrug resistance in K562 cell line by a novel synthetic calmodulin inhibitor, E6. Biol Pharm Bull 2005;28:1974 – 8.

29. Lebedeva IV, Su ZZ, Chang Y, Kitada S, Reed JC, Fisher PB. The cancer growth suppressing gene *mda*-7 induces apoptosis selectively in human melanoma cells. Oncogene 2002;21:708 – 18.

30. Lebedeva IV, Su ZZ, Sarkar D, et al. Melanoma differentiation associated gene-7, *mda*-7/interleukin-24, induces apoptosis in prostate cancer cells by promoting mitochondrial dysfunction and inducing reactive oxygen species. Cancer Res 2003;63:8138 – 44.

31. Endicott JA, Ling V. The biochemistry of P-glycoprotein-mediated multidrug resistance. Annu Rev Biochem 1989;58:137 – 71.

32. Gottesman MM, Fojo T, Bates SE. Multidrug resistance in cancer: role of ATP-dependent transporters. Nat Rev 2002;2:48 – 58.

33. Ludwig JA, Szakacs G, Martin SE, et al. Selective toxicity of NSC73306 in MDR1-positive cells as a new strategy to circumvent multidrug resistance in cancer. Cancer Res 2006;66:4808 – 15.

34. Lebedeva IV, Su ZZ, Emdad L, et al. Targeting inhibition of K-ras enhances Ad *mda*-7-induced growth suppression and apoptosis in mutant K-ras colorectal cancer cells. Oncogene 2007;26:733 – 44.

35. Jacobson MD. Reactive oxygen species and programmed cell death. Trends Biochem Sci 1996;21:83 – 6.

36. Yacoub A, Mitchell C, Brannon J, et al. MDA-7 (interleukin-24) inhibits the proliferation of renal carcinoma cells and interacts with free radicals to promote cell death and loss of reproductive capacity. Mol Cancer Ther 2003;2:623 – 32.

37. Zamzami N, Marchetti P, Castedo M, et al. Sequential reduction of mitochondrial transmembrane potential and generation of reactive oxygen species in early programmed cell death. J Exp Med 1995;182:367 – 77.

38. Calcabrini A, Arancia G, Marra M, et al. Enzymatic oxidation products of spermine induce greater cytotoxic effects on human multidrug-resistant colon carcinoma cells (LoVo) than on their wild-type counterparts. Int J Cancer 2002;99:43 – 52.

39. Park SJ, Wu CH, Choi MR, Najafi F, Emami A, Safa AR. P-glycoprotein enhances TRAIL-triggered apoptosis in multidrug resistant cancer cells by interacting with the death receptor DR5. Biochem Pharmacol 2006;72: 293 – 307.

40. Bergman AM, Munch-Petersen B, Jensen PB, et al. Collateral sensitivity to gemcitabine (2′,2′ difluorodeoxycytidine) and cytosine arabinoside of daunorubicin- and VM-26-resistant variants of human small cell lung cancer cell lines. Biochem Pharmacol 2001;61:1401 – 8.

41. Jia L, Kelsey SM, Grahn MF, Jiang XR, Newland AC. Increased activity and sensitivity of mitochondrial respiratory enzymes to tumor necrosis factor α-mediated inhibition is associated with increased cytotoxicity in drug-resistant leukemic cell lines. Blood 1996;87:2401 – 10.

42. Jia L, Allen PD, Macey MG, Grahn MF, Newland AC, Kelsey SM. Mitochondrial electron transport chain activity, but not ATP synthesis, is required for drug-induced apoptosis in human leukaemic cells: a possible novel mechanism of regulating drug resistance. Br J Haematol 1997;98: 686 – 98.

43. Hao JH, Yu M, Liu FT, Newland AC, Jia L. Bcl-2 inhibitors sensitize tumor necrosis factor-related apoptosis-inducing ligand-induced apoptosis by uncoupling of mitochondrial respiration in human leukemic CEM cells. Cancer Res 2004;64:3607 – 16.